DOI: 10.1002/num.22827

RESEARCH ARTICLE

WILEY

Unconditionally stable exponential time differencing schemes for the mass-conserving Allen–Cahn equation with nonlocal and local effects

Kun Jiang^{1,2} | Lili Ju³ | Jingwei Li⁴ | Xiao Li⁵

Correspondence

Lili Ju, Department of Mathematics, University of South Carolina, Columbia, SC 29208, USA. Email: ju@math.sc.edu

Funding information

National Natural Science Foundation of China, Grant/Award Numbers: 11801024, 61962056; US National Science Foundation, Grant/Award Numbers: DMS-1818438, DMS-2109633.

Abstract

It is well known that the classic Allen-Cahn equation satisfies the maximum bound principle (MBP), that is, the absolute value of its solution is uniformly bounded for all time by certain constant under suitable initial and boundary conditions. In this paper, we consider numerical solutions of the modified Allen-Cahn equation with a Lagrange multiplier of nonlocal and local effects, which not only shares the same MBP as the original Allen-Cahn equation but also conserves the mass exactly. We reformulate the model equation with a linear stabilizing technique, then construct first- and second-order exponential time differencing schemes for its time integration. We prove the unconditional MBP preservation and mass conservation of the proposed schemes in the time discrete sense and derive their error estimates under some regularity assumptions. Various numerical experiments in two and three dimensions are also conducted to verify the theoretical results.

KEYWORDS

Allen–Cahn equation, exponential time differencing, linear stabilization, mass-conserving, maximum bound principle

1 | INTRODUCTION

The classic Allen–Cahn equation takes the following form:

$$\partial_t u(\mathbf{x}, t) = \varepsilon^2 \Delta u(\mathbf{x}, t) + f(u(\mathbf{x}, t)), \qquad \mathbf{x} \in \Omega, \ t > 0,$$
 (1)

 ¹School of Mathematics and Statistics, Qilu University of Technology, Jinan, China
 ²Faculty of Science, Beijing University of Technology, Beijing, China
 ³Department of Mathematics, University of South Carolina, Columbia, South Carolina, USA
 ⁴Laboratory of Mathematics and Complex Systems and School of Mathematical Science, Beijing Normal University, Beijing, China
 ⁵Department of Applied Mathematics, The Hong Kong Polytechnic University, Kowloon, Hong Kong

where $u(\mathbf{x},t)$ is the real-valued unknown function, $\Omega \subset \mathbb{R}^d$ (d=2,3) is an open, connected and bounded domain with the Lipschitz continuous boundary $\partial \Omega$, ε is an interfacial parameter and f(u) = -F'(u) with F(u) being certain nonlinear potential function. The classic Allen–Cahn equation can be regarded as the L^2 gradient flow with respect to the energy functional

$$E[u(\mathbf{x},t)] := \int_{\Omega} \left(\frac{\varepsilon^2}{2} |\nabla u(\mathbf{x},t)|^2 + F(u(\mathbf{x},t)) \right) d\mathbf{x}, \tag{2}$$

and its solution satisfies the energy dissipation law as follows:

$$\frac{d}{dt}E[u(\mathbf{x},t)] \le 0. \tag{3}$$

The Allen–Cahn equation was originally introduced by Allen and Cahn [1] as a model for the phase separation process of a binary alloy under a fixed temperature. Since then the Allen–Cahn equation has been intensively studied due to its connection to the celebrated curvature driven geometric flow. In the past few decades, many works on the Allen–Cahn equation have been devoted to motions of interfaces, especially, motion by mean curvature, and numerous applications ranging from image processing [2, 3], material sciences [1] to biology [4].

Many parabolic types of equations often satisfy an important property, that is, the solution must reach its maximum and/or minimum either at the initial time or on the boundary of the domain, which is the well-studied maximum principle [5]. The Allen–Cahn Equation (1) satisfies a similar property, called the maximum bound principle (MBP) [6, 7]: if the initial data and/or the boundary values are pointwise bounded by a certain constant in absolute value, then the absolute value of the solution is also bounded by the same constant everywhere and for all time. For example, when the double-well potential $F(u) = \frac{1}{4}(u^2 - 1)^2$ (and $f(u) = -F'(u) = u - u^3$) is used, the constant bounding the solution is 1, that is, $||u(\cdot,t)|| \le 1$ for all $t \ge 0$ if $||u(\cdot,0)|| \le 1$, where $||\cdot||$ denotes the supremum norm. The MBP is weaker than the conventional maximum principle in the sense that a problem satisfying a maximum principle must satisfy an MBP. The Equation (1) with a uniformly elliptic linear operator L replacing $\varepsilon^2 \Delta$ and f = 0 satisfies the maximum principle. There have also been many studies devoted to maximum principle preserving numerical approximations of linear elliptic operators, such as finite difference method [8, 9], lumped-mass finite element method [10, 11], collocation method [12, 13], and finite volume method [14]. For the Equation (1) with a uniformly elliptic linear operator, the nonlinear term f(u) leads to the existence of time-invariant regions [7], in which the MBP was proved as a special invariant region of the Allen–Cahn equation. Recently, a variety of works have been done on whether such an MBP could be preserved by some time-stepping schemes for discretizing the Allen-Cahn equation. The discrete MBPs of a finite difference semi-discrete scheme and its fully discrete approximations with forward and backward Euler time-stepping methods were obtained in one-dimensional space [15]. Moreover, the first-order stabilized implicit-explicit schemes with finite difference spatial discretization were proved to preserve the MBP [16], which was then generalized [17] to the case with more general nonlinear terms.

The Cahn–Hilliard equation, a fourth-order equation governed by the same energy functional (2), satisfies the so-called mass conservation while the Allen–Cahn equation fails to satisfy this property. One can modify the Allen–Cahn equation to satisfy the mass conservation by adding an extra Lagrange term of nonlocal constraint as [18]

$$\partial_t u(\mathbf{x}, t) = \varepsilon^2 \Delta u(\mathbf{x}, t) + f(u(\mathbf{x}, t)) - \frac{1}{|\Omega|} \int_{\Omega} f(u(\mathbf{y}, t)) d\mathbf{y}, \qquad \mathbf{x} \in \Omega, \ t > 0.$$
 (4)

Integrating both sides of the Equation (4) over Ω , we can see that the modified Allen–Cahn Equation (4) conserves the total mass exactly:

$$\frac{d}{dt} \int_{\Omega} u(\mathbf{x}, t) d\mathbf{x} = 0,$$

or equivalently, $\int_{\Omega} u(\mathbf{x}, t) d\mathbf{x} = \int_{\Omega} u(\mathbf{x}, 0) d\mathbf{x}$. In addition, the solution to the modified Allen–Cahn Equation (4) also satisfies the same energy dissipation laws [18] (3) as the classic Allen–Cahn Equation (1). However, a drawback of such modification is that the value of the solution to (4) may fall beyond the interval [-1, 1] even for the commonly used double-well potential case [18, 19].

Apart from the Equation (4), for the Allen–Cahn equation with the double-well potential, another well-known modification is to impose a Lagrange multiplier [20] as follows:

$$\partial_t u(\mathbf{x}, t) = \varepsilon^2 \Delta u(\mathbf{x}, t) + f(u(\mathbf{x}, t)) - \frac{\int_{\Omega} f(u(\mathbf{y}, t)) \, d\mathbf{y}}{\int_{\Omega} \sqrt{4F(u(\mathbf{y}, t))} \, d\mathbf{y}} \sqrt{4F(u(\mathbf{x}, t))}, \qquad \mathbf{x} \in \Omega, \quad t > 0, \quad (5)$$

where $f(u) = u - u^3$ and $F(u) = \frac{1}{4}(1 - u^2)^2$. It is easy to show that the total mass is also exactly conserved for (5). Furthermore, the conservation of mass is ensured by the nonlocal effect of the Lagrange multiplier $-\frac{1}{|\Omega|} \int_{\Omega} f(u) \, d\mathbf{y}$ in (4), whereas the Lagrange multiplier in (5) combines both nonlocal and local effects. Alfaro and Alifrangis have proven that the solution to (5) satisfies the same MBP [21] as that for the classic Allen–Cahn Equation (1), that is, $||u(\cdot,t)|| \le 1$ for all $t \ge 0$ if $||u(\cdot,0)|| \le 1$. However, the dissipation law with respect to the original energy functional (2) does not hold theoretically for the Equation (5); instead, the Equation (5) is the L^2 gradient flow with respect to a slightly different energy functional modified from (2) [20].

There have been quite a few researches denoted to numerical schemes for the mass-conserving Allen–Cahn Equation (4). Kim et al. [22] proposed a practically unconditionally stable hybrid scheme with an exact mass-conserving update at each time step. Zhai et al. [23, 24] proposed the Crank–Nicolson and operator splitting schemes. Lee [25] discretized the equation by using a Fourier spectral method in space and first-, second-, and third-order implicit explicit Runge–Kutta schemes in time.

Recently, the exponential time differencing (ETD) (or say, the exponential integrator) has been considered for constructing unconditionally MBP-preserving schemes for the classic Allen-Cahn equation. The ETD method comes from the variation-of-constants formula with the nonlinear terms approximated by polynomial interpolations, followed by exact integration of the resulting integrals. The ETD schemes have been systematically studied [26] and further developed by Cox and Matthews for the applications to stiff systems [27]. Hochbruck and Ostermann provided several nice reviews on ETD Runge-Kutta method [28] and ETD multistep method [29] for semilinear parabolic problems and the convergence of these methods were analyzed. Du and Zhu [30, 31] investigated the linear stabilities of some ETD and modified ETD schemes for the Allen-Cahn equation in two- and three-dimensional spaces. One advantage of the ETD schemes is the exact evaluation of the linear part so that they possess good stability and accuracy even though the linear terms have strong stiffness. Thus, ETD schemes have been successfully applied to phase-field models which often yield highly stiff ODE systems under suitable spatial discretization. Some high-order numerical methods based on fast and stable ETD schemes were developed for solving the Allen–Cahn equation [32], the Cahn–Hilliard equation [33], the elastic bending energy model [34], and the no-slope-selection thin film equation [35, 36]. A localized compact ETD method was firstly presented [37] for time integration with large step sizes for phase-field simulations of coarsening dynamics on the Sunway TaihuLight supercomputer. In addition, MBP-preserving numerical schemes have been also studied for the fractional Allen-Cahn equation with the Crank-Nicolson time-stepping [38], the nonlocal Allen-Cahn equation by using

first- and second-order ETD schemes [39], and the conservative Allen–Cahn Equation (4) using the ETD schemes [19]. In a very recent work, an abstract framework was established [6] for analyzing the MBPs of semilinear parabolic equations and unconditionally MBP-preserving ETD schemes, and it was claimed that the classic ETD methods with order higher than 2 cannot preserve the MBP unconditionally. Several third- and fourth-order MBP-preserving schemes were developed for the Allen–Cahn equation by considering the integrating factor Runge–Kutta schemes [40–42]. An arbitrarily high-order ETD multistep method was presented in Reference [43] by enforcing the maximum bound via an extra cutoff postprocessing.

In this paper, we are interested in developing stable linear schemes for solving the mass-conserving Allen–Cahn Equation (5) based on the ETD approach. The rest of the paper is organized as follows. In Section 2, we first reformulate the model Equation (5) based on the linear stabilizing technique, and then propose first- and second-order ETD schemes for time integration of the transformed equation, which are shown to be unconditionally mass-conserved and MBP-preserving in the time discrete sense. In Section 3, we prove the convergence of the proposed ETD schemes under certain regularity assumptions. Various numerical experiments in two and three dimensions are performed in Section 4 to validate the theoretical results. Finally, some concluding remarks are drawn in Section 5.

2 | UNCONDITIONALLY MBP-PRESERVING EXPONENTIAL TIME DIFFERENCING SCHEMES

Let us restate the mass-conserving Allen–Cahn equation with local and nonlocal effects as follows:

$$\partial_t u(\mathbf{x}, t) = \varepsilon^2 \Delta u(\mathbf{x}, t) + \overline{f}[u](\mathbf{x}, t), \qquad \mathbf{x} \in \Omega, \ t > 0,$$
 (6)

with

$$\bar{f}[u](\mathbf{x},t) = f(u(\mathbf{x},t)) - \frac{\int_{\Omega} f(u(\mathbf{y},t)) \, \mathrm{d}\mathbf{y}}{\int_{\Omega} g(u(\mathbf{y},t)) \, \mathrm{d}\mathbf{y}} g(u(\mathbf{x},t)). \tag{7}$$

where $f(u) = u - u^3$ and $g(u) = \sqrt{4F(u)} = 1 - u^2$ (the notation of absolute value is dropped off since $1 - u^2 \ge 0$ due to the MBP in the time–space continuous setting), subject to the initial value condition

$$u(\mathbf{x}, 0) = u_0(\mathbf{x}), \qquad \mathbf{x} \in \overline{\Omega},$$
 (8)

for some $u_0 \in C(\overline{\Omega})$ with $\overline{\Omega} = \Omega \cup \partial \Omega$. We impose either the periodic boundary condition (such as a regular rectangular domain $\Omega = \prod_{i=1}^d (a_i, b_i)$) or homogeneous Neumann boundary condition given by

$$\frac{\partial u(\mathbf{x},t)}{\partial \mathbf{n}} = 0, \quad \mathbf{x} \in \partial \Omega, \ t \ge 0,$$

where **n** is the outer unit normal vector on the boundary $\partial\Omega$. Integrating both sides of the Equation (6) over Ω , it is easy to verify its mass-conserving property:

$$\int_{\Omega} u(\mathbf{x}, t) \, d\mathbf{x} = M_0 := \int_{\Omega} u_0(\mathbf{x}) \, d\mathbf{x}, \quad t \ge 0.$$

The nonlinear functions f and g are continuously differentiable and

$$f(-1) = f(1) = 0, \quad g(-1) = g(1) = 0.$$
 (9)

The MBP property with the bounding constant 1 then becomes a result of the invariant set for the Equation (6) [21]. In addition, the two constant functions $u(\cdot,t) \equiv 1$ or $u(\cdot,t) \equiv -1$ are clearly trivial solutions to the Equation (6). Hence we always assume that $||u_0|| \leq 1$ and $|M_0| \neq |\Omega|$ (i.e., $u_0 \not\equiv \pm 1$) to avoid the these two trivial solution cases.

In comparison with the original Allen–Cahn equation, the modified Allen–Cahn Equation (6) can preserve the mass conservation by introducing the local and nonlocal Lagrange multiplier. However, the energy dissipation law does not hold with respect to the original energy functional (2). To the best of our knowledge, the mass-conserving Allen–Cahn Equation (6) with the double-well potential function has been proved to possess the MBP [21], while whether or not the MBP also holds for the logarithmic potential case or other forms is still an open question. Therefore, in this paper we only focus on studying the unconditional MBP-preserving schemes for the double-well potential function case.

2.1 | Linear splitting for stabilization

Let us define

$$\lambda_u(t) = \frac{\int_{\Omega} f(u(\mathbf{x}, t)) \, d\mathbf{x}}{\int_{\Omega} g(u(\mathbf{x}, t)) \, d\mathbf{x}},\tag{10}$$

then we can write the Equation (6) as

$$\partial_t u(\mathbf{x}, t) = \varepsilon^2 \Delta u(\mathbf{x}, t) + f(u(\mathbf{x}, t)) - \lambda_u(t) g(u(\mathbf{x}, t)). \tag{11}$$

Next we present a result on the boundedness of $\lambda_u(t)$.

Lemma 1 For any function $\xi \in C(\overline{\Omega})$ with $\|\xi\| \le 1$ and $\xi \not\equiv \pm 1$, it holds that

$$|\lambda_{\xi}| \le 1. \tag{12}$$

Proof. Since $\|\xi\| \le 1$ we have $g(\xi(\mathbf{x})) = 1 - \xi^2(\mathbf{x}) \ge 0$ for any $\mathbf{x} \in \overline{\Omega}$. Furthermore, it is clear $\int_{\Omega} g(\xi(\mathbf{x})) \, d\mathbf{x} > 0$ since $\xi \in C(\overline{\Omega})$ and $\xi \not\equiv \pm 1$. Thus we have

$$\begin{split} |\lambda_{\xi}| &= \left| \frac{\int_{\Omega} f(\xi(\mathbf{x})) \, \mathrm{d}\mathbf{x}}{\int_{\Omega} g(\xi(\mathbf{x})) \, \mathrm{d}\mathbf{x}} \right| = \frac{\left| \int_{\Omega} \xi(\mathbf{x}) - \xi(\mathbf{x})^3 \, \mathrm{d}\mathbf{x} \right|}{\int_{\Omega} 1 - \xi(\mathbf{x})^2 \, \mathrm{d}\mathbf{x}} \\ &\leq \frac{\int_{\Omega} \|\xi\| (1 - \xi(\mathbf{x})^2) \, \mathrm{d}\mathbf{x}}{\int_{\Omega} 1 - \xi(\mathbf{x})^2 \, \mathrm{d}\mathbf{x}} = \|\xi\| \leq 1, \end{split}$$

which completes the proof.

Remark 2 Note that for any function $\xi \in C(\overline{\Omega})$ with $\|\xi\| \le 1$, the condition $\xi \not\equiv \pm 1$ is equivalent to $|\int_{\Omega} \xi(\mathbf{x}) \, d\mathbf{x}| \neq |\Omega|$. In the case of the constant functions $\xi \equiv \pm 1$, the above result can be understood in the limit sense. The boundedness of $\lambda_u(t)$ plays an important role in ensuring that the solutions to the mass-conserving Allen–Cahn Equation (6) and the corresponding temporally discretized equation analyzed later are always located in the interval [-1, 1].

Next, let us introduce the stabilizing constant $\kappa > 0$. Correspondingly, the mass-conserving Allen–Cahn Equation (6) can be written in the following equivalent form

$$\partial_t u(\mathbf{x}, t) = \mathcal{L}_{\kappa} u(\mathbf{x}, t) + \mathcal{N}[u](\mathbf{x}, t), \qquad \mathbf{x} \in \Omega, \ t > 0,$$
(13)

where the linear operator

$$\mathcal{L}_{\kappa} = \varepsilon^2 \Delta - \kappa \mathcal{I}$$

and the nonlinear term

$$\mathcal{N}[u](\mathbf{x},t) = \kappa u(\mathbf{x},t) + \overline{f}[u](\mathbf{x},t)$$

= $\kappa u(\mathbf{x},t) + f(u(\mathbf{x},t)) - \lambda_u(t)g(u(\mathbf{x},t)).$

We require that the stabilizing constant κ always satisfies

$$\kappa \ge \max_{|\xi| \le 1} (|f'(\xi)| + |g'(\xi)|) = \max_{|\xi| \le 1} (|1 - 3\xi^2| + |-2\xi|) = 2 + 2 = 4, \tag{14}$$

Then we have the following lemma on the nonlinear term.

Lemma 2 Suppose that the requirement (14) holds. For any function $\xi \in C(\overline{\Omega})$ with $\|\xi\| \le 1$ and $\xi \not\equiv \pm 1$, we have

$$\|\mathcal{N}[\xi]\| \le \kappa. \tag{15}$$

Proof. For any $\xi \in C(\overline{\Omega})$ such that $||\xi|| \le 1$, we have from [6] that

$$0 \le \kappa + f'(\xi(\mathbf{x})) - \lambda_{\xi} g'(\xi(\mathbf{x})) \le 2\kappa, \quad \forall \mathbf{x} \in \overline{\Omega}, \tag{16}$$

where we have used the result $\|\lambda_{\xi}\| \le 1$ guaranteed by Lemma 2.1. Then, the combination of (9) and (16) yields

$$-\kappa = -\kappa + f(-1) - \lambda_{\xi} g(-1) \le \mathcal{N}[\xi](\mathbf{x}) = \kappa \xi(\mathbf{x}) + f(\xi(\mathbf{x})) - \lambda_{\xi} g(\xi(\mathbf{x}))$$
$$\le \kappa + f(1) - \lambda_{\xi} g(1) = \kappa \tag{17}$$

for any $\mathbf{x} \in \overline{\Omega}$, which completes the proof.

2.2 | Exponential time differencing for time integration

Now we propose and analyze first- and second-order linear schemes for time integration of the mass-conserving Allen–Cahn Equation (6) based on the equivalent form (13) and the exponential time differencing approach.

Let us divide the time interval by $\{t_n = n\tau\}_{n\geq 0}$ with a time step size $\tau > 0$. The essence of the ETD method is to approximate the nonlinear operator $\mathcal{N}[u]$ by some interpolation. We define $w(\mathbf{x}, s) = u(\mathbf{x}, t_n + s)$ for $s \in [0, \tau]$, then we have the following problem:

$$\begin{cases} \partial_{s} w = \mathcal{L}_{\kappa} w + \mathcal{N}[w], & \mathbf{x} \in \Omega, s \in (0, \tau], \\ w(\mathbf{x}, 0) = u(\mathbf{x}, t_{n}), & \mathbf{x} \in \overline{\Omega}, \end{cases}$$
(18)

equipped with the periodic boundary condition or homogeneous Neumann boundary condition.

Setting $\mathcal{N}[u(t_n + s)] \approx \mathcal{N}[u(t_n)]$ in (18) gives the first-order ETD (ETD1) scheme: for $n \ge 0$ and given u^n , find $u^{n+1} = w^n(\tau)$ solving

$$\begin{cases} \partial_{s} w^{n} = \mathcal{L}_{\kappa} w^{n} + \mathcal{N}[u^{n}], & \mathbf{x} \in \Omega, s \in (0, \tau], \\ w^{n}(\mathbf{x}, 0) = u^{n}, & \mathbf{x} \in \overline{\Omega}, \end{cases}$$
(19)

subject to the periodic or homogeneous Neumann boundary condition, where u^n represents an approximation of $u(t_n)$ and $u^0 = u_0(\cdot)$ is given.

First we have the following lemma regarding the Laplace operator.

Lemma 3 [6] For any $w \in \{u \in C(\Omega) \mid \Delta u \in C(\Omega)\}$ and $\mathbf{x}_0 \in \Omega$, if

$$w(\mathbf{x}_0) = \max_{\mathbf{x} \in \overline{\Omega}} w(\mathbf{x}),$$

then $\Delta w(\mathbf{x}_0) \leq 0$. The Laplace operator Δ , enforced by the periodic or homogeneous Neumann boundary condition, generates a contraction semigroup $\{e^{\Delta t}\}_{t\geq 0}$ with respect

to the supremum norm on the subspace of $C(\overline{\Omega})$ [6], and for any $\alpha \geq 0$, it holds that

$$||e^{t(\Delta-\alpha)}u|| \le e^{-\alpha t}||u||, \quad t \ge 0,$$
(20)

for any $u \in C(\overline{\Omega})$.

Proposition 1 (Mass conservation of the ETD1 scheme) The ETD1 Scheme (19) conserves the mass unconditionally, i.e., for any time step size $\tau > 0$, the ETD1 solution satisfies

$$\int_{\Omega} u^n \, \mathrm{d}\mathbf{x} = M_0, \quad \forall n \ge 0. \tag{21}$$

Proof. By induction, assuming that $\int_{\Omega} u^n d\mathbf{x} = M_0$ is given, we only need to show $\int_{\Omega} u^{n+1} d\mathbf{x} = M_0$. Taking the L^2 inner product of (19) with 1, we immediately obtain

$$\frac{d}{ds} \int_{\Omega} w^n \, d\mathbf{x} + \kappa \int_{\Omega} w^n \, d\mathbf{x} = \kappa \int_{\Omega} u^n \, d\mathbf{x} = \kappa M_0.$$

Let $V(s) = \int_{\Omega} w^n(s) d\mathbf{x}$, then we have

$$\frac{dV(s)}{ds} + \kappa V(s) = \kappa M_0,$$

with $V(0) = M_0$. Multiplying by the exponential term $e^{\kappa s}$ and integrating on the interval $[0, \tau]$, we immediately get

$$V(\tau)e^{\kappa\tau} - M_0 = M_0(e^{\kappa\tau} - 1),$$

which implies $\int_{\Omega} u^{n+1} d\mathbf{x} = V(\tau) = M_0$.

Proposition 1 implies that if $u_0 \not\equiv \pm 1$ (i.e., $|M_0| \neq |\Omega|$), then $u^n \not\equiv \pm 1$ for any $n \geq 0$.

Theorem 1 (Discrete MBP of the ETD1 scheme) Suppose that the requirement (14) holds and $||u_0|| \le 1$ with $|M_0| \ne |\Omega|$. Then the ETD1 Scheme (19) preserves the discrete MBP unconditionally, i.e., for any time step size $\tau > 0$, the ETD1 solution satisfies $||u^n|| \le 1$ for any $n \ge 0$.

Proof. By induction, we just need to show that $||u^n|| \le 1$ and $u^n \not\equiv \pm 1$ deduce $||u^{n+1}|| \le 1$ for any n. The integration form of the ETD1 Scheme (19) reads as

$$u^{n+1} = e^{\tau \mathcal{L}_{\kappa}} u^n + \int_0^{\tau} e^{(\tau - s)\mathcal{L}_{\kappa}} \mathcal{N}[u^n] \, \mathrm{d}s. \tag{22}$$

According to Lemmas 2 and 3 and $||u^n|| \le 1$, we obtain

$$||u^{n+1}|| \le ||e^{\tau \mathcal{L}_{\kappa}}|| ||u^{n}|| + \int_{0}^{\tau} ||e^{(\tau - s)\mathcal{L}_{\kappa}}|| ||\mathcal{N}[u^{n}]|| ds$$

$$\le e^{-\kappa \tau} + \int_{0}^{\tau} e^{-(\tau - s)\kappa} \kappa \, ds$$

$$= e^{-\kappa \tau} + \kappa \frac{1 - e^{-\kappa \tau}}{\kappa} = 1,$$

which completes the proof.

Remark 3 By approximating $e^{-\tau \mathcal{L}_{\kappa}} \approx \mathcal{I} - \tau \mathcal{L}_{\kappa}$ in the ETD1 Scheme (22), one can obtain

$$\frac{u^{n+1}-u^n}{\tau}=\mathcal{L}_{\kappa}u^{n+1}+\mathcal{N}[u^n],$$

which is exactly the standard stabilized implicit-explicit Euler (IMEX1) scheme, linear, and also preserves the MBP [16] unconditionally. Such an observation suggests that the IMEX1 scheme is actually an approximation of the ETD1 scheme, and the ETD1 solution is more accurate since it preserves completely the exponential behavior of the linear operator and partially the nonlinear term [32, 33] while the IMEX1 scheme only uses the first-order leading term.

The second-order ETD scheme of Runge–Kutta (ETDRK2) type is given by: find $u^{n+1} = w^n(\tau)$ solving

$$\begin{cases} \partial_{s}w^{n} = \mathcal{L}_{\kappa}w^{n} + \left(1 - \frac{s}{\tau}\right)\mathcal{N}[u^{n}] + \frac{s}{\tau}\mathcal{N}[\widetilde{u}^{n+1}], & \mathbf{x} \in \Omega, \ s \in (0, \tau], \\ w^{n}(x, 0) = u^{n}, & \mathbf{x} \in \overline{\Omega}, \end{cases}$$
(23)

with $u^0 = u_0(\cdot)$, subject to the periodic or homogeneous Neumann boundary condition, where \widetilde{u}^{n+1} is generated by the ETD1 Scheme (19). It is worth noting that both ETD1 and ETDRK2 schemes are linear. We now prove the mass conservation and the discrete MBP for the ETDRK2 scheme.

Proposition 2 (Mass conservation of the ETDRK2 scheme) The ETDRK2 Scheme (23) conserves the mass unconditionally, i.e., for any time step size $\tau > 0$, the ETDRK2 solution satisfies

$$\int_{\Omega} u^n \, \mathrm{d}\mathbf{x} = M_0, \quad \forall n \ge 0. \tag{24}$$

Proof. Similar to the proof for Proposition 1, by taking the L^2 inner product with (23) by 1, we have

$$\frac{d}{ds} \int_{\Omega} w^n \, d\mathbf{x} + \kappa \int_{\Omega} w^n \, d\mathbf{x} = \left(1 - \frac{s}{\tau}\right) \kappa \int_{\Omega} u^n \, d\mathbf{x} + \frac{s}{\tau} \kappa \int_{\Omega} \widetilde{u}^{n+1} \, d\mathbf{x} = \kappa M_0,$$

where we have used $\int_{\Omega} \widetilde{u}^{n+1} d\mathbf{x} = M_0$ from Proposition 1. Thus we obtain $\int_{\Omega} u^{n+1} d\mathbf{x} = M_0$, which completes the proof.

Theorem 2 (Discrete MBP of the ETDRK2 scheme) Suppose that the requirement (14) holds, $||u_0|| \le 1$ with $|M_0| \ne |\Omega|$. Then the ETDRK2 Scheme (23) preserves the discrete MBP unconditionally, i.e., for any time step size $\tau > 0$, the ETDRK2 solution satisfies $||u^n|| \le 1$ for any n > 0.

Proof. By induction, let us assume that $||u^n|| \le 1$ and $u^n \not\equiv \pm 1$ for some n. From the ETDRK2 Scheme (23), we have

$$u^{n+1} = e^{\tau \mathcal{L}_{\kappa}} u^n + \int_0^{\tau} e^{(\tau - s)\mathcal{L}_{\kappa}} \left[\left(1 - \frac{s}{\tau} \right) \mathcal{N}[u^n] + \frac{s}{\tau} \mathcal{N}[\widetilde{u}^{n+1}] \right] ds. \tag{25}$$

According to Lemmas 2-3, $||u^n|| \le 1$ and $||\widetilde{u}^{n+1}|| \le 1$ (by Theorem 1), we obtain

$$||u^{n+1}|| \le ||e^{\tau \mathcal{L}_{\kappa}}|| ||u^{n}|| + \int_{0}^{\tau} ||e^{(\tau - s)\mathcal{L}_{\kappa}}|| \left[\left(1 - \frac{s}{\tau} \right) ||\mathcal{N}[u^{n}]|| + \frac{s}{\tau} ||\mathcal{N}[\widetilde{u}^{n+1}]|| \right] ds$$

$$\leq e^{-\kappa\tau} + \int_0^{\tau} e^{-\kappa(\tau - s)} \left[\left(1 - \frac{s}{\tau} \right) \kappa + \frac{s}{\tau} \kappa \right] ds$$
$$= e^{-\kappa\tau} + \kappa \frac{1 - e^{-\kappa\tau}}{\kappa} = 1,$$

which completes the proof.

Remark 4 Different from the IMEX1 scheme, it was shown in Reference [42] that the IMEX Runge–Kutta schemes with order greater than 1 only preserves the MBP conditionally; more precisely, their MBP preservation still has the constraint on the time step size and the spatial mesh size.

Remark 5 As claimed in Reference [6], the classic ETD Runge–Kutta approximations with order greater than 2 fail to maintain the MBP unconditionally since the higher-order interpolation polynomials contain negative coefficients, and this also happens to the mass-conserving Allen–Cahn Equation (6). In addition to the Runge–Kutta type approach, multistep methods have also been widely used to design high-order schemes for gradient flow models, such as the third-order ETD multistep scheme and the BDF3 scheme for the no-slope-selection thin film model [36, 44]. However, the ETD multistep approach is based on the extrapolation for the nonlinear term. Due to the existence of negative coefficients, the extrapolation polynomials cannot be bounded by the maxima and minima of the extrapolated data, and thus the resulting ETD multistep schemes with order greater than 1 fail to unconditionally preserve the MBP [6]. More recently, the integrating factor Runge–Kutta (IFRK) method was considered for time integrartion of the classic Allen–Cahn equation in References [40, 41], which successfully gives some high-order MBP-preserving schemes, thus it remains very interesting to apply them to the mass-conserving Allen–Cahn Equation (6).

2.3 | Fully discrete schemes

In the following, we briefly discuss the fully discrete ETD schemes corresponding to (19) and (23), which are also unconditionally MBP preserving. To this end, we recall the continuity of a function defined on a set $D \subset \mathbb{R}^d$ as [45]:

w is continuous at
$$\mathbf{x}^* \in D \Leftrightarrow \forall \mathbf{x}_k \to \mathbf{x}^* \text{ in } D \text{ implies } w(\mathbf{x}_k) \to w(\mathbf{x}^*).$$

Thus, under the same theoretical framework, the MBP property of the mass-conserving Allen–Cahn Equation (6) can be further extended to the case of finite-dimensional operators in space, such as replacing Δ by its discrete approximation denoted by Δ_h . As shown in Reference [6], it is easy to verify that the central difference operator and lumped-mass finite element operator for spatial discretization of the Laplace operator Δ also satisfy Lemma 3. In this case, Δ_h can be simply regarded as a square matrix and generates a contraction semigroup $\{e^{\Delta_h t}\}_{t\geq 0}$ on the subspace of C(X) satisfying the periodic or homogeneous Neumann boundary condition, where X is the set of all spacial grid points (boundary and interior points). The resulting space-discrete equation of (6) with Δ replaced by Δ_h becomes an ordinary differential equation (ODE) system taking the same form:

$$u_t = \varepsilon^2 \Delta_h u + \bar{f}[u], \quad \mathbf{x} \in X^*, t > 0$$

with $u(\mathbf{x}, 0) = u_0(\mathbf{x})$ for any $\mathbf{x} \in X$, where $X^* = X$ for the homogeneous Neumann boundary condition and $X^* = X \cap \overline{\Omega}^+$ with $\overline{\Omega}^+ = \prod_{i=1}^d (a_i, b_i]$ for the periodic boundary condition.

We present below the formulas of the fully-discrete ETD1 and ETDRK2 schemes, which can be directly implemented for computation. Let $\mathcal{L}_{\kappa,h} = \varepsilon^2 \Delta_h - \kappa \mathcal{I}$ and define the ϕ -functions as follows:

$$\phi_0(a) = e^a,$$
 $\phi_1(a) = \frac{e^a - 1}{a},$
 $\phi_2(a) = \frac{e^a - 1 - a}{a^2},$

for any $a \neq 0$. Then the fully-discrete ETD1 scheme is given by

$$u^{n+1} = e^{\tau \mathcal{L}_{\kappa,h}} u^n + \int_0^{\tau} e^{(\tau - s) \mathcal{L}_{\kappa,h}} \mathcal{N}[u^n] \, \mathrm{d}s,$$

or equivalently,

$$u^{n+1} = \phi_0(\tau \mathcal{L}_{\kappa,h})u^n + \tau \phi_1(\tau \mathcal{L}_{\kappa,h})\mathcal{N}[u^n], \tag{26}$$

and the fully-discrete ETDRK2 scheme by

$$\begin{cases} \widetilde{u}^{n+1} = e^{\tau \mathcal{L}_{\kappa,h}} u^n + \int_0^{\tau} e^{(\tau - s) \mathcal{L}_{\kappa,h}} \mathcal{N}[u^n] \, \mathrm{d}s, \\ u^{n+1} = e^{\tau \mathcal{L}_{\kappa,h}} u^n + \int_0^{\tau} e^{(\tau - s) \mathcal{L}_{\kappa,h}} \left\{ \left(1 - \frac{s}{\tau} \right) \mathcal{N}[u^n] + \frac{s}{\tau} \mathcal{N}[\widetilde{u}^{n+1}] \right\} \, \mathrm{d}s, \end{cases}$$

or equivalently,

$$\begin{cases}
\widetilde{u}^{n+1} = \phi_0(\tau \mathcal{L}_{\kappa,h})u^n + \tau \phi_1(\tau \mathcal{L}_{\kappa,h})\mathcal{N}[u^n], \\
u^{n+1} = \widetilde{u}^{n+1} + \tau \phi_2(\tau \mathcal{L}_{\kappa,h})(\mathcal{N}[\widetilde{u}^{n+1}] - \mathcal{N}[u^n]).
\end{cases}$$
(27)

3 | ERROR ESTIMATES

In the following, we carry out convergence analysis for the ETD Schemes (19) and (23) in the space-continuous setting. We first derive some useful results as follows.

Lemma 4 Let γ be any constant such that $|\Omega| > \gamma > 0$. For any $\xi_1, \xi_2 \in C(\overline{\Omega})$ with $\|\xi_i\| \le 1$ and $\int_{\Omega} g(\xi_i(\mathbf{x}, t)) d\mathbf{x} \ge \gamma$ (i = 1, 2), we have

$$\|\lambda_{\xi_1} g(\xi_1) - \lambda_{\xi_2} g(\xi_2)\| \le C_{\gamma} \|\xi_1 - \xi_2\|, \tag{28}$$

where $C_{\gamma} = \frac{4|\Omega|}{\gamma} + \frac{2|\Omega|^2}{\gamma^2}$.

Proof. We first have for any $\mathbf{x} \in \overline{\Omega}$,

$$\begin{split} \lambda_{\xi_1} g(\xi_1(\mathbf{x})) - \lambda_{\xi_2} g(\xi_2((\mathbf{x})) &= \frac{\int_{\Omega} f(\xi_1(\mathbf{y})) \, \mathrm{d}\mathbf{y}}{\int_{\Omega} g(\xi_1(\mathbf{y})) \, \mathrm{d}\mathbf{y}} g(\xi_1(\mathbf{x})) - \frac{\int_{\Omega} f(\xi_2(\mathbf{y})) \, \mathrm{d}\mathbf{y}}{\int_{\Omega} g(\xi_2(\mathbf{y})) \, \mathrm{d}\mathbf{y}} g(\xi_2(\mathbf{x})) \\ &= \left(\int_{\Omega} f(\xi_1(\mathbf{y})) - f(\xi_2(\mathbf{y})) \, \mathrm{d}\mathbf{y}\right) \frac{g(\xi_1(\mathbf{x}))}{\int_{\Omega} g(\xi_1(\mathbf{y})) \, \mathrm{d}\mathbf{y}} \\ &+ \int_{\Omega} f(\xi_2(\mathbf{y})) \, \mathrm{d}\mathbf{y} \left(\frac{g(\xi_1(\mathbf{x}))}{\int_{\Omega} g(\xi_1(\mathbf{y})) \, \mathrm{d}\mathbf{y}} - \frac{g(\xi_2(\mathbf{x}))}{\int_{\Omega} g(\xi_2(\mathbf{y})) \, \mathrm{d}\mathbf{y}}\right) \\ &= \left(\int_{\Omega} f(\xi_1(\mathbf{y})) - f(\xi_2(\mathbf{y})) \, \mathrm{d}\mathbf{y}\right) \frac{g(\xi_1(\mathbf{x}))}{\int_{\Omega} g(\xi_1(\mathbf{y})) \, \mathrm{d}\mathbf{y}} \end{split}$$

$$+ \left(\int_{\Omega} f(\xi_{2}(\mathbf{y})) \, d\mathbf{y} \right) \frac{g(\xi_{1}(\mathbf{x})) - g(\xi_{2}(\mathbf{x}))}{\int_{\Omega} g(\xi_{2}(\mathbf{y})) \, d\mathbf{y}}$$

$$+ \int_{\Omega} f(\xi_{2}(\mathbf{y})) \, d\mathbf{y} \left(g(\xi_{1}(\mathbf{x})) \frac{\int_{\Omega} g(\xi_{2}(\mathbf{y})) - g(\xi_{1}(\mathbf{y})) \, d\mathbf{y}}{\int_{\Omega} g(\xi_{1}(\mathbf{y})) \, d\mathbf{y} \int_{\Omega} g(\xi_{2}(\mathbf{y})) \, d\mathbf{y}} \right)$$

$$=: I_{1} + I_{2} + I_{3}.$$

Notice that $|g(\xi(\mathbf{x}))| \le 1$, $|f(\xi(\mathbf{x}))| \le 1$, $|g'(\xi(\mathbf{x}))| \le 2$, and $|f'(\xi(\mathbf{x}))| \le 2$ for any $\xi \in C(\overline{\Omega})$ with $||\xi|| \le 1$, then we get

$$\begin{split} |I_{1}| &\leq \frac{1}{\gamma} |g(\xi_{1}(\mathbf{x}))| \int_{\Omega} |f(\xi_{1}(\mathbf{y})) - f(\xi_{2}(\mathbf{y}))| \, \mathrm{d}\mathbf{y} \leq \frac{2|\Omega|}{\gamma} ||\xi_{1} - \xi_{2}||, \\ |I_{2}| &\leq \frac{|\Omega|}{\gamma} ||f(\xi_{2})|| |g(\xi_{2}(\mathbf{x})) - g(\xi_{1}(\mathbf{x}))| \leq \frac{2|\Omega|}{\gamma} ||\xi_{1} - \xi_{2}||, \\ |I_{3}| &\leq \frac{|\Omega|}{\gamma^{2}} ||f(\xi_{2})|| |g(\xi_{1}(\mathbf{x}))| \int_{\Omega} |g(\xi_{2}(\mathbf{y})) - g(\xi_{1}(\mathbf{y}))| \, \mathrm{d}\mathbf{y} \leq \frac{2|\Omega|^{2}}{\gamma^{2}} ||\xi_{1} - \xi_{2}||. \end{split}$$

By combining the above results, we obtain

$$\|\lambda_{\xi_1} g(\xi_1) - \lambda_{\xi_2} g(\xi_2)\| \le \left(\frac{4|\Omega|}{\gamma} + \frac{2|\Omega|^2}{\gamma^2}\right) \|\xi_1 - \xi_2\|,\tag{29}$$

which completes the proof.

Lemma 5 Suppose that the requirement (14) holds and let γ be any constant such that $|\Omega| > \gamma > 0$. For any $\xi_1, \xi_2 \in C(\overline{\Omega})$ with $||\xi_i|| \le 1$ and $\int_{\Omega} g(\xi_i(\mathbf{x}, t)) d\mathbf{x} \ge \gamma$ (i = 1, 2), we have

$$\|\mathcal{N}[\xi_1] - \mathcal{N}[\xi_2]\| \le C_{\gamma}^* \kappa \|\xi_1 - \xi_2\|,\tag{30}$$

where $C_{\gamma}^{*} = \frac{3}{2} + \frac{C_{\gamma}}{4}$.

Proof. It is easy to check that for any $\mathbf{x} \in \overline{\Omega}$,

$$\begin{split} |\mathcal{N}[\xi_{1}](\mathbf{x}) - \mathcal{N}[\xi_{2}](\mathbf{x})| &= |\kappa(\xi_{1}(\mathbf{x}) - \xi_{2}(\mathbf{x})) + (f(\xi_{1}(\mathbf{x})) - f(\xi_{2}(\mathbf{x})) - (\lambda_{\xi_{1}}g(\xi_{1}(\mathbf{x})) - \lambda_{\xi_{2}}g(\xi_{2}(\mathbf{x})))| \\ &\leq \kappa|\xi_{1}(\mathbf{x}) - \xi_{2}(\mathbf{x})| + |f(\xi_{1}(\mathbf{x})) - f(\xi_{2}(\mathbf{x}))| + |\lambda_{\xi_{1}}g(\xi_{1}(\mathbf{x})) - \lambda_{\xi_{2}}g(\xi_{2}(\mathbf{x}))| \\ &\leq (\kappa + 2 + C_{\gamma})||\xi_{1} - \xi_{2}|| \\ &\leq \left(\frac{3}{2} + \frac{C_{\gamma}}{4}\right)\kappa||\xi_{1} - \xi_{2}||, \end{split}$$

where we have used Lemma 4 and the requirement $\kappa \geq 4$. The proof is completed.

Next, we study the convergence for the ETD Schemes (19) and (23). Let T > 0 be a given fixed terminal time. For any $u \in C([0,T];C(\overline{\Omega}))$ with $||u(t)|| \le 1$ and $\int_{\Omega} u(\mathbf{x},t) \, d\mathbf{x} = M_0 \ne |\Omega|$ for any $t \in [0,T]$, there always exists a constant $\gamma_u > 0$ such that $\int_{\Omega} g(u(\mathbf{x},t)) \, d\mathbf{x} \ge \gamma_u$ for any $t \in [0,T]$ due to the continuity and boundedness of u.

Theorem 3 (Error estimate of the ETD1 scheme) Suppose that the requirement (14) holds and $||u_0|| \le 1$ with $|M_0| \ne |\Omega|$. Assume that the exact solution u to the model problem (6) belongs to $C^1([0,T];C(\overline{\Omega}))$ and let $\{u^n \in C(\overline{\Omega})\}_{n\ge 0}$ be the approximate solution generated by the ETD1 Scheme (19). Furthermore, we also assume that there

exists a constant $\gamma_d > 0$ such that $\int_{\Omega} g(u^n(\mathbf{x})) d\mathbf{x} \ge \gamma_d$ for any n with $n\tau \le T$ and define $\gamma = \min(\gamma_u, \gamma_d)$. Then we have

$$||u(t_n) - u^n|| \le \frac{C_{\gamma}^*}{C_{\gamma}^* - 1} C e^{(C_{\gamma}^* - 1)\kappa t_n} \tau, \quad \forall t_n \le T,$$
 (31)

for any $\tau > 0$, where the constant C > 0 is independent of τ , γ and κ .

Proof. Let $e_1^n = u^n - u(t_n)$. The difference between (19) and (18) yields

$$e_1^{n+1} = e^{\mathcal{L}_{\kappa}\tau} e_1^n + \int_0^{\tau} e^{\mathcal{L}_{\kappa}(\tau - s)} \{ \mathcal{N}[u^n] - \mathcal{N}[u(t_n)] + R_1(s) \} \, \mathrm{d}s, \tag{32}$$

where $R_1(s)$ is the truncation error as

$$R_1(s) = \mathcal{N}[u(t_n)] - \mathcal{N}[u(t_n + s)], \quad s \in [0, \tau].$$

By the MBP property of *u* and Lemma 5, we have

$$||R_1(s)|| = ||\mathcal{N}[u(t_n)] - \mathcal{N}[u(t_n + s)]|| \le C_{\gamma}^* \kappa ||u(t_n) - u(t_n + s)|| \le C_1 C_{\gamma}^* \kappa \tau, \quad \forall s \in [0, \tau],$$

where the constant C_1 depends on the $C^1([0,T];C(\overline{\Omega})$ norm of u, but independent of τ and κ . Similarly, since $||u^n|| \le 1$ due to Theorem 1, we also obtain by Lemma 5 that

$$\|\mathcal{N}[u^n] - \mathcal{N}[u(t_n)]\| \le C_{\gamma}^* \kappa \|u^n - u(t_n)\| = C_{\gamma}^* \kappa \|e_1^n\|. \tag{33}$$

Then, we derive from (32) and Lemma 3 that

$$||e_{1}^{n+1}|| \leq e^{-\kappa\tau} ||e_{1}^{n}|| + \int_{0}^{\tau} e^{-\kappa(\tau-s)} \{||\mathcal{N}[u^{n}] - \mathcal{N}[u(t_{n})]|| + ||R_{1}(s)||\} ds$$

$$\leq e^{-\kappa\tau} ||e_{1}^{n}|| + C_{\gamma}^{*}\kappa(||e_{1}^{n}|| + C_{1}\tau) \int_{0}^{\tau} e^{-\kappa(\tau-s)} ds$$

$$= e^{-\kappa\tau} ||e_{1}^{n}|| + \frac{1 - e^{-\kappa\tau}}{\kappa} C_{\gamma}^{*}\kappa(||e_{1}^{n}|| + C_{1}\tau)$$

$$= (C_{\gamma}^{*} - (C_{\gamma}^{*} - 1)e^{-\kappa\tau}) ||e_{1}^{n}|| + \frac{1 - e^{-\kappa\tau}}{\kappa\tau} C_{\gamma}^{*}C_{1}\kappa\tau^{2}$$

$$\leq (1 + (C_{\gamma}^{*} - 1)\kappa\tau) ||e_{1}^{n}|| + C_{\gamma}^{*}C_{1}\kappa\tau^{2},$$
(34)

where in the last step we have used the fact that $1 - e^{-a} \le a$ for any a > 0. By induction, we have

$$\begin{aligned} \|e_1^n\| &\leq (1 + (C_\gamma^* - 1)\kappa\tau)^n \|e_1^0\| + C_\gamma^* C_1 \kappa\tau^2 \sum_{k=0}^{n-1} (1 + (C_\gamma^* - 1)\kappa\tau)^k \\ &= (1 + (C_\gamma^* - 1)\kappa\tau)^n \|e_1^0\| + \frac{C_\gamma^* C_1}{C_\gamma^* - 1} \tau [(1 + (C_\gamma^* - 1)\kappa\tau)^n - 1] \\ &\leq \mathrm{e}^{(C_\gamma^* - 1)\kappa n\tau} \|e_1^0\| + \frac{C_\gamma^*}{C_\gamma^* - 1} C_1 \mathrm{e}^{(C_\gamma^* - 1)\kappa n\tau} \tau. \end{aligned}$$

Finally we obtain (31) by letting $C = C_1$ since $e_1^0 = 0$ and $n\tau = t_n$.

Theorem 4 (Error estimate of the ETDRK2 scheme) Suppose that the requirement (14) holds and $||u_0|| \le 1$ with $|M_0| \ne |\Omega|$. Assume that the exact solution u to the model problem (6) belongs to $C^2([0,T];C(\overline{\Omega}))$ and let $\{u^n \in C(\overline{\Omega})\}_{n\ge 0}$ be the approximate solution generated by the ETD2 Scheme (23). Furthermore, we also assume that there

exists a constant $\gamma_d > 0$ such that $\int_{\Omega} g(u^n(\mathbf{x})) d\mathbf{x} \ge \gamma_d$ for any n with $n\tau \le T$ and define $\gamma = \min(\gamma_u, \gamma_d)$. Then we have

$$||u(t_n) - u^n|| \le Ce^{(C_{\gamma}^* - 1)\kappa t_n} \tau^2, \quad \forall t_n \le T,$$
 (35)

for any $\tau > 0$, where the constant C > 0 is independent of τ .

Proof. The proof strategy is quite similar to that for the ETD1 scheme. Let $e_2^n = u^n - u(t_n)$, then we have

$$e_{2}^{n+1} = e^{\mathcal{L}_{\kappa}\tau} e_{2}^{n} + \int_{0}^{\tau} e^{\mathcal{L}_{\kappa}(\tau-s)} \left\{ \left(1 - \frac{s}{\tau}\right) \left(\mathcal{N}[u^{n}] - \mathcal{N}[u(t_{n})]\right) + \frac{s}{\tau} \left(\mathcal{N}[\widetilde{u}^{n+1}] - \mathcal{N}[u(t_{n+1})]\right) + R_{2}(s) \right\} ds,$$
(36)

where $R_2(s)$ is the truncation error given by

$$R_2(s) = \left(1 - \frac{s}{\tau}\right) \mathcal{N}[u(t_n)] + \frac{s}{\tau} \mathcal{N}[u(t_{n+1})] - \mathcal{N}[u(t_n + s)], \quad s \in [0, \tau].$$

Using the estimation of the linear interpolation, we have

$$||R_2(s)|| \le C_2 \tau^2, \quad \forall s \in [0, \tau],$$

where the constant C_2 depends on the $C^2([0, T], C(\overline{\Omega}))$ norm of u and γ but is independent of τ . From the last inequality in (34), we know

$$\|\widetilde{u}^{n+1} - u(t_{n+1})\| \le (1 + (C_{\gamma}^* - 1)\kappa\tau)\|u^n - u(t_n)\| + C_{\gamma}^* C_1 \kappa \tau^2.$$

By combining the above inequality with Theorem 2 and Lemma 5, we have, for any $s \in [0, \tau]$,

$$\begin{split} & \left\| \left(1 - \frac{s}{\tau} \right) (\mathcal{N}[u^n] - \mathcal{N}[u(t_n)]) + \frac{s}{\tau} (\mathcal{N}[\widetilde{u}^{n+1}] - \mathcal{N}[u(t_{n+1})]) \right\| \\ & \leq C_{\gamma}^* \kappa \left(\left(1 - \frac{s}{\tau} \right) \|e_2^n\| + \frac{s}{\tau} ((1 + (C_{\gamma}^* - 1)\kappa\tau) \|e_2^n\| + C_{\gamma}^* C_1 \kappa \tau^2) \right) \\ & = C_{\gamma}^* \kappa \|e_2^n\| + C_{\gamma}^* (C_{\gamma}^* - 1)\kappa^2 s \|e_2^n\| + C_{\gamma}^{*2} C_1 \kappa^2 \tau s. \end{split}$$

Then, we obtain from (36) and Lemma 3 that

$$\begin{split} \|e_{2}^{n+1}\| & \leq \mathrm{e}^{-\kappa\tau} \|e_{2}^{n}\| + \int_{0}^{\tau} \mathrm{e}^{-\kappa(\tau-s)} \{C_{\gamma}^{*}\kappa \|e_{2}^{n}\| + C_{\gamma}^{*}(C_{\gamma}^{*}-1)\kappa^{2}s \|e_{2}^{n}\| + C_{\gamma}^{*2}C_{1}\kappa^{2}\tau s + C_{2}\tau^{2}\} \, \mathrm{d}s \\ & = \mathrm{e}^{-\kappa\tau} \|e_{2}^{n}\| + (C_{\gamma}^{*}\kappa \|e_{2}^{n}\| + C_{2}\tau^{2}) \int_{0}^{\tau} \mathrm{e}^{-\kappa(\tau-s)} \, \mathrm{d}s \\ & + (C_{\gamma}^{*}(C_{\gamma}^{*}-1)\kappa^{2} \|e_{2}^{n}\| + C_{\gamma}^{*2}C_{1}\kappa^{2}\tau) \int_{0}^{\tau} s \mathrm{e}^{-\kappa(\tau-s)} \, \mathrm{d}s \\ & = \mathrm{e}^{-\kappa\tau} \|e_{2}^{n}\| + \frac{1-\mathrm{e}^{-\kappa\tau}}{\kappa} (C_{\gamma}^{*}\kappa \|e_{2}^{n}\| + C_{2}\tau^{2}) \\ & + \frac{\mathrm{e}^{-\kappa\tau}-1+\kappa\tau}{\kappa^{2}} (C_{\gamma}^{*}(C_{\gamma}^{*}-1)\kappa^{2} \|e_{2}^{n}\| + C_{\gamma}^{*2}C_{1}\kappa^{2}\tau) \\ & = ((C_{\gamma}^{*}-1)^{2}\mathrm{e}^{-\kappa\tau} + C_{\gamma}^{*}(C_{\gamma}^{*}-1)\kappa\tau - C_{\gamma}^{*}(C_{\gamma}^{*}-2)) \|e_{2}^{n}\| \\ & + \frac{1-\mathrm{e}^{-\kappa\tau}}{\kappa} C_{2}\tau^{2} + \frac{\mathrm{e}^{-\kappa\tau}-1+\kappa\tau}{\kappa^{2}} \cdot C_{\gamma}^{*2}C_{1}\kappa^{2}\tau \\ & \leq \left(1+(C_{\gamma}^{*}-1)\kappa\tau + \frac{1}{2}(C_{\gamma}^{*}-1)^{2}(\kappa\tau)^{2}\right) \|e_{2}^{n}\| + \left(C_{2} + \frac{1}{2}C_{\gamma}^{*}C_{1}\kappa^{2}\right)\tau^{3}, \end{split}$$

where we have used the inequality $1 - a \le e^{-a} \le 1 - a + \frac{a^2}{2}$ for any a > 0. By induction, we obtain

$$\begin{split} \|e_2^n\| & \leq \left(1 + (C_\gamma^* - 1)\kappa\tau + \frac{1}{2}(C_\gamma^* - 1)^2(\kappa\tau)^2\right)^n \|e_2^0\| \\ & + \left(\frac{1}{2}C_\gamma^*C_1\kappa^2 + C_2\right)\tau^3 \sum_{k=0}^{n-1} \left(1 + (C_\gamma^* - 1)\kappa\tau + \frac{1}{2}(C_\gamma^* - 1)^2(\kappa\tau)^2\right)^k \\ & \leq \left(1 + (C_\gamma^* - 1)\kappa\tau + \frac{1}{2}(C_\gamma^* - 1)^2(\kappa\tau)^2\right)^n \|e_2^0\| \\ & + \left(\frac{C_\gamma^*}{2(C_\gamma^* - 1)}C_1\kappa + \frac{C_2}{(C_\gamma^* - 1)\kappa}\right)\tau^2\left(\left(1 + (C_\gamma^* - 1)\kappa\tau + \frac{1}{2}(C_\gamma^* - 1)^2(\kappa\tau)^2\right)^n - 1\right) \\ & \leq \mathrm{e}^{(C_\gamma^* - 1)\kappa n\tau} \|e_2^0\| + \left(\frac{C_\gamma^*}{2(C_\gamma^* - 1)}C_1\kappa + \frac{C_2}{(C_\gamma^* - 1)\kappa}\right)\mathrm{e}^{(C_\gamma^* - 1)\kappa n\tau}\tau^2. \end{split}$$

By letting
$$C = \frac{C_{\gamma}^*}{2(C_{\gamma}^* - 1)}C_1\kappa + \frac{C_2}{(C_{\gamma}^* - 1)\kappa}$$
, we finally obtain (35) since $e_2^0 = 0$ and $n\tau = t_n$.

Remark 6 In Theorems 3 and 4, we additionally assume that there exists a constant $\gamma_d > 0$ such that $\int_\Omega g(u^n(\mathbf{x})) \, d\mathbf{x} \ge \gamma_d$ for any n with $n\tau \le T$. While this assumption on the approximate solution $\{u^n\}$ is necessary to our current proofs of the error estimates, it remains an interesting question whether such assumption can be removed with other analysis techniques. Here, we only give the temporal convergence analysis for the ETD1 and ETDRK2 schemes in the space-continuous setting. In the similar spirit of the analysis in Reference [39], the convergence analysis for the fully discrete version is also available by taking the truncation error for spatial discretization into account.

4 | NUMERICAL EXPERIMENTS

In this section, we present some numerical experiments to demonstrate the performance (convergence rates, mass conservation and MBP preservation) of the proposed ETD Schemes (19) and (23) for the mass-conserving Allen–Cahn Equation (6). We take the domain $\Omega = (-0.5,0.5)^d$ with d=2 or 3. Moreover, the ETDRK2 scheme is used in all examples while the ETD1 scheme is only considered in temporal convergence tests due to its lack of high accuracy. For simplicity, we here only consider the case of periodic boundary condition and the case of homogeneous Neumann boundary condition is similar. The stabilizing coefficient is set to be $\kappa=4$ in all experiments. The spatial discretization is performed by the central difference discretization to form the fully-discrete Schemes (26) and (27), in which the products of matrix exponentials with vectors are computed using the fast Fourier transform based implementation [32].

4.1 | Convergence tests

We run the first- and second-order ETD schemes for the mass-conserving Allen–Cahn Equation (6) in 2D with $\varepsilon = 0.01$ and the initial value $u_0(x, y) = \cos(2\pi x)\cos(2\pi y)$. The terminal time is chosen to be T = 1. In order to accurately catch the convergence rate in time, the spatial mesh size must be small enough and we set h = 1/1024. To compute the solution errors under different time step sizes $\tau = 1/2^k$ for k = 2, 3, ..., 8, we treat the approximate solution obtained by the ETDRK2 scheme with $\tau = 1/1024$ as the benchmark. Table 1 reports the L^{∞} and L^2 norms of the solution errors

1/256

5.43e - 3

1.20

3.33e - 3

	ETD1				ETDRK2					
τ	L^2 error	Rate	L^{∞} error	Rate	L^2 error	Rate	L^{∞} error	Rate		
1/4	2.28e-1		1.51e-1		1.49e-1		9.57e-2			
1/8	1.57e-1	0.54	1.01e-1	0.58	6.98e-2	1.09	4.36e-2	1.13		
1/16	9.40e-2	0.74	5.95e-2	0.77	2.53e-2	1.47	1.55e-2	1.49		
1/32	5.12e-2	0.87	3.19e-2	0.90	7.72e-3	1.71	4.69e-3	1.72		
1/64	2.61e-2	0.97	1.61e-2	0.98	2.13e-3	1.85	1.29e-3	1.86		
1/128	1.25e-2	1.06	7.70e-3	1.06	5.57e-4	1.94	3.37e-4	1.94		

TABLE 1 L^2 and L^∞ solution errors at T=1 and corresponding convergence rates in time by the ETD1 and ETDRK2 schemes respectively

TABLE 2 L^2 and L^{∞} solution errors at T=1 and corresponding convergence rates in space by the ETDRK2 scheme

1.20

1.36e - 4

2.03

8.23e - 5

2.03

h	L ² error	Rate	L^{∞} error	Rate
1/64	9.98e-4		3.14e-4	
/128	3.09e-4	1.69	9.21e-5	1.77
/256	8.38e-5	1.88	2.40e-5	1.94
/512	2.12e-5	1.97	6.07e-6	1.98
/1024	5.33e-6	1.99	1.52e-6	1.99

at the terminal time T=1 and corresponding temporal convergence rates, which clearly verifies the first-order temporal accuracy for ETD1 and the second-order temporal accuracy for ETDRK2 respectively.

Next, we test the spatial convergence of the central difference using the ETDRK2 scheme. We fix the time step size $\tau = T/1024$ and regard the approximate solution produced by the ETDRK2 scheme with h = 1/2048 as the benchmark for computing the solution errors with different spatial mesh sizes. The L^{∞} and L^2 norms of the solution errors at T = 1 and corresponding convergence rates are presented in Table 2. It is observed that the convergence rates with respect to h are clearly of second order as expected.

4.2 Tests of mass-conservation and MBP-preservation

We numerically simulate and investigate the discrete MBP in long-time phase separation processes governed by the mass-conserving Allen–Cahn Equation (6) in 2D and 3D spaces. The ETDRK2 scheme is used. We set $\varepsilon=0.01$ and the time step size $\tau=0.1$. The spatial grid size is selected to be h=1/1024 in 2D and h=1/256 in 3D .

We start the 2D simulations with an initial configuration of $u_0 = 0.9$ rand (·) (here rand (·) represents the quasi-uniform random distribution between -1 and 1). In this case, we also compare the simulation results with those produced by the classic Cahn–Hilliard equation [33]

$$\partial_t u(\mathbf{x}, t) = -\Delta(\varepsilon^2 \Delta u(\mathbf{x}, t) + f(u(\mathbf{x}, t))), \qquad \mathbf{x} \in \Omega, \ t > 0,$$
(37)

with $\varepsilon = 0.01$ and the same initial configuration. Figure 1 presents the configurations of the simulated solutions at t = 1, 100, 1000, and 2500 for the mass-conserving Allen–Cahn Equation (6). The steady state is gradually reached after about t = 2000. The evolutions of the mass, the supremum norm

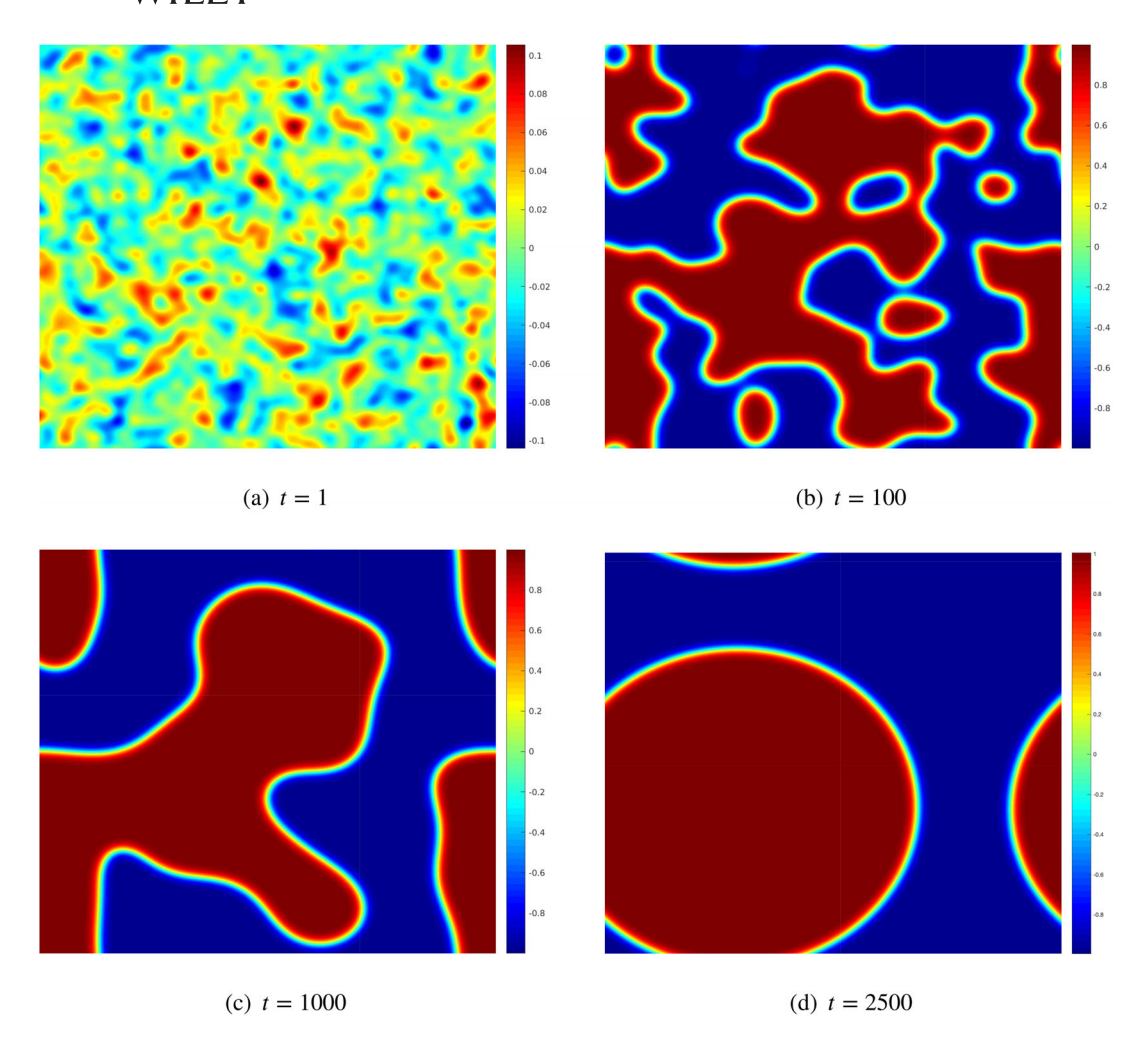


FIGURE 1 The simulated solutions at t = 1, 100, 1000, and 2500, respectively, for the mass-conserving Allen–Cahn equation with an initial quasi-uniform state in 2D by the ETDRK2 scheme

and the energy are plotted in Figure 2. It is easy to see that the mass is exactly conserved and the discrete MBP is preserved perfectly along the time. Although there is no energy dissipation law for the Equation (6) theoretically, we still observe that the energy decays monotonically for this example. The configurations of the simulated solutions at t = 1, 10, 50, and 300 for the Cahn–Hilliard equation are presented in Figure 3, where the same steady state is reached after around t = 80. This implies that the evolution of the phase structure in the mass-conserving Allen–Cahn equation is much slower than that in the Cahn–Hilliard equation. Figure 4 shows the corresponding evolutions of the mass, the supremum norm and the energy. We observe that the mass is conserved and the energy decays monotonically along the time. However, the supremum norm of the numerical solution is beyond the constant 1 after about t = 1 since the Cahn–Hilliard equation does not have the MBP property.

Our 3D simulations start with the quasi-uniform initial state $u_0 = 0.9 \, \text{rand}(\cdot)$ as well. Figure 5 presents the configurations of the computed solution at t = 1, 30, 200, and 4000 for the mass-conserving Allen–Cahn equation. The corresponding evolutions of the mass, the supremum norm and the energy are plotted in Figure 6. We observed again that the mass is exactly conserved, the discrete MBP is preserved perfectly, and the energy decays monotonically along the time.

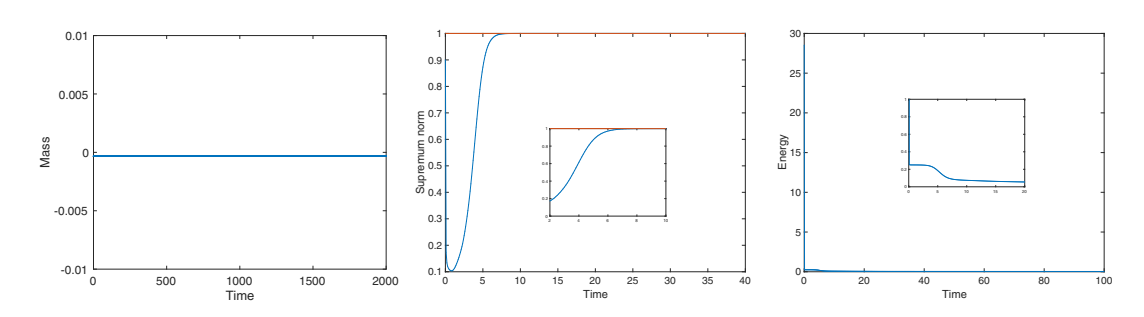


FIGURE 2 Evolutions of the mass, the supremum norm and the energy of the simulated solutions for the mass-conserving Allen–Cahn equation with an initial quasi-uniform state in 2D by the ETDRK2 scheme

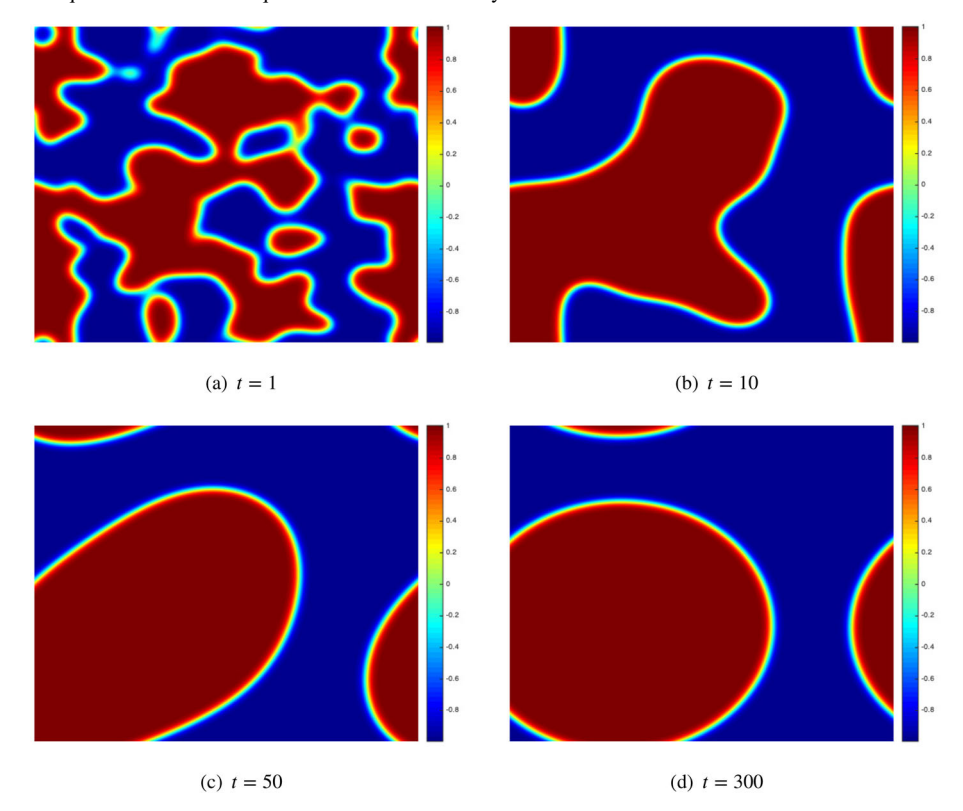


FIGURE 3 The simulated solution at t = 1, 10, 50, and 300, respectively, for the Cahn–Hilliard equation with an initial quasi-uniform state in 2D

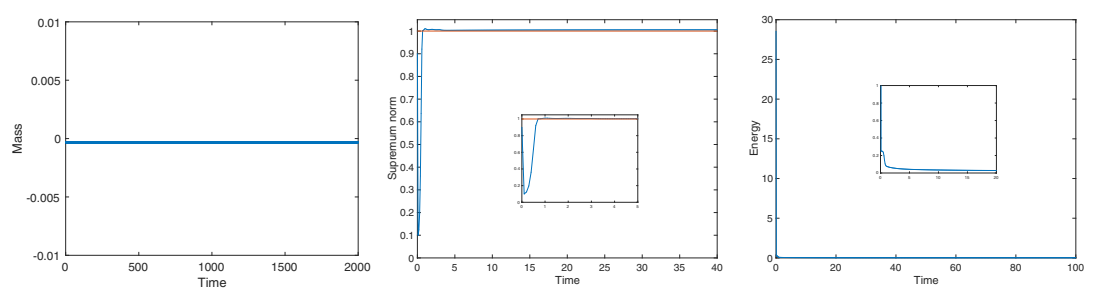


FIGURE 4 Evolutions of the mass, the supremum norm and the energy of the simulated solutions for the Cahn–Hilliard equation with an initial quasi-uniform state in 2D

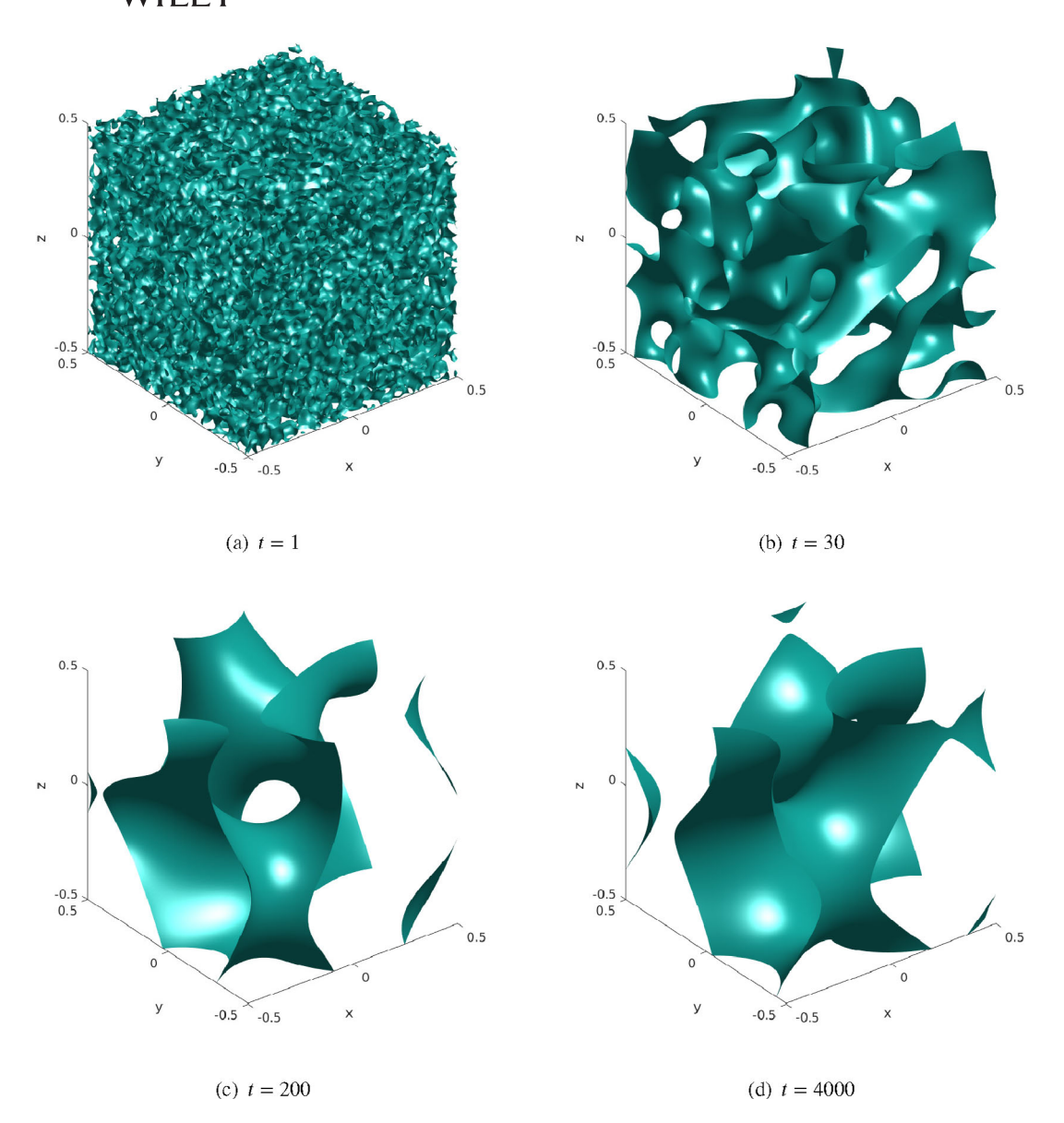


FIGURE 5 The simulated phase structures at t = 1, 30, 200, and 4000 respectively for the mass-conserving Allen–Cahn equation with an initial quasi-uniform state in 3D

4.3 | The expanding bubble test

We use the ETDRK2 scheme to simulate the expansion process of the bubble in 3D, governed by the mass-conserving Allen–Cahn equation beginning with a discontinuous initial configuration

$$u_0 = \begin{cases} -0.5, & x^2 + y^2 + z^2 < 0.25^2, \\ 0.5, & \text{otherwise.} \end{cases}$$
 (38)

The temporal and spatial step size are set as $\tau = 0.1$ and h = 1/256. Figure 7 presents the simulated process of the expanding bubble, that is, the isosurface views of the numerical solutions at t = 1, 10, 15, and 100, respectively. Figure 8 illustrates the evolutions of the mass, the supremum norm, the

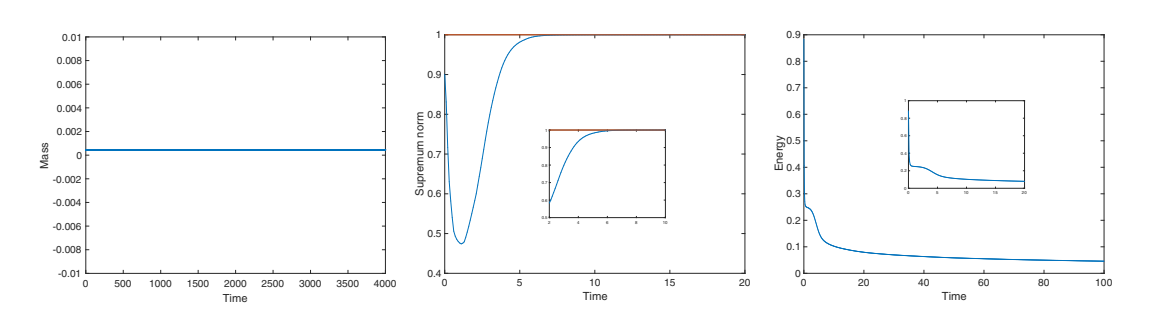


FIGURE 6 Evolutions of the mass, the supremum norm and the energy of the simulated solutions for the mass-conserving Allen–Cahn equation with an initial quasi-uniform state in 3D

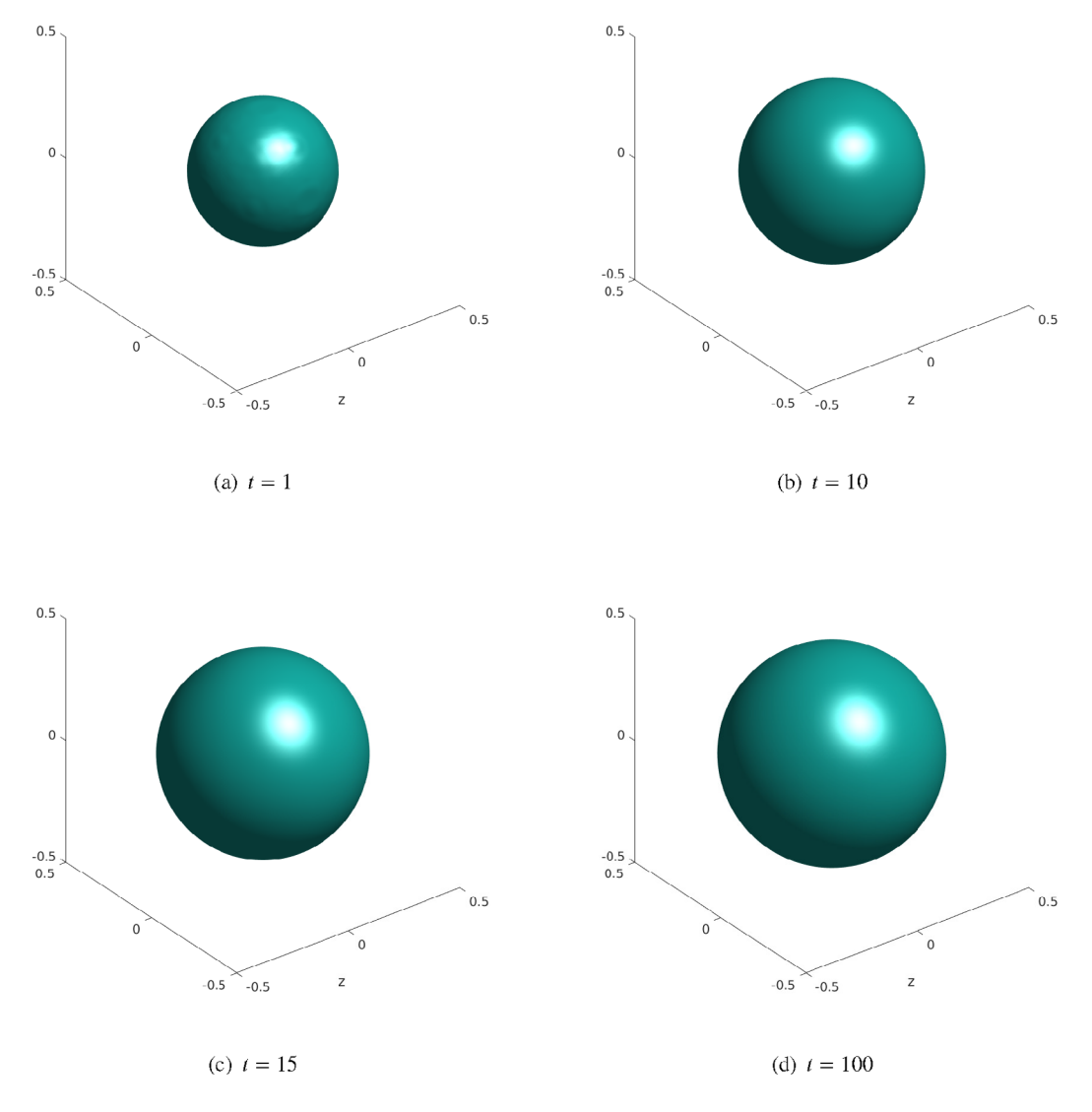


FIGURE 7 The simulated phase structures at t = 1, 10, 15, and 100, respectively, for the expanding bubble test in 3D

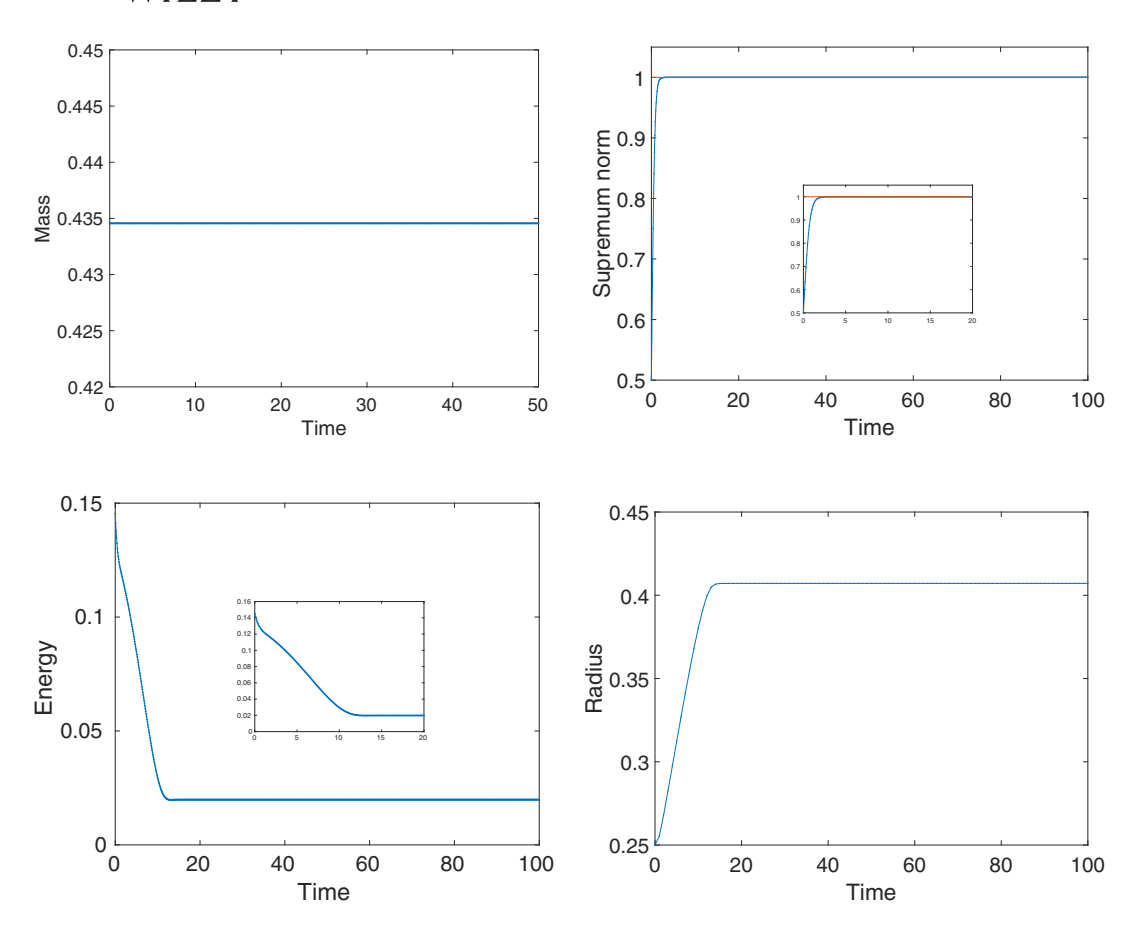


FIGURE 8 Evolutions of the mass, the supremum norm, the energy and the radius of the simulated solutions for the expanding bubble test in 3D

energy and the radius of the bubble along the time. It is again observed that the mass is conserved, the discrete MBP is well preserved, and the energy decays monotonically. The radius of the bubble increases monotonically and the steady state is reached (a bubble with radius $r \approx 0.407$ as expected [19]) after about t = 18.

5 | CONCLUSIONS

In this paper, we propose and analyze first- and second- order linear schemes for solving the mass-conserving Allen–Cahn equation with local and nonlocal effects (in the double-well potential case), which are based on the combination of the linear stabilizing technique and the exponential time differencing method. We prove that the proposed schemes are unconditionally MBP-preserving and mass-conserved in the time-discrete sense. Error estimates of these schemes are also rigorously derived under some assumptions. It remains an open problem whether a more delicate analysis can relieve the extra assumption on the numerical solutions $\{u^n\}$ in Theorems 3 and 4 as discussed in Remark 6. In addition, it is worth mentioning that the Flory-Huggins potential is also widely-used in the classic Allen–Cahn model and how to extend the current work to that case is subject to future investigation as well.

ACKNOWLEDGMENTS

L. Ju's work is partially supported by U.S. National Science Foundation under Grant Numbers DMS-1818438 and DMS-2109633. J. Li's work is partially supported by National Natural Science Foundation of China under Grant Number 61962056. X. Li's work is partially supported by National Natural Science Foundation of China under Grant Number 11801024.

DATA AVAILABILITY STATEMENT

Data sharing not applicable to this article as no datasets were generated or analysed during the current study.

ORCID

Lili Ju https://orcid.org/0000-0002-6520-582X

REFERENCES

- [1] S. M. Allen and J. W. Cahn, A microscopic theory for antiphase boundary motion and its application to antiphase domain coarsening, Acta Metall. 27 (1979), 1084–1095.
- [2] F. Catté, F. Dibos, and G. Koepfler, A morphological scheme for mean curvature motion and applications to anisotropic diffusion and motion of level sets, SIAM J. Numer. Anal. 32 (1995), 1895–1909.
- [3] K. Pope and S. T. Acton, *Modified mean curvature motion for multispectral anisotropic diffusion*, IEEE Proc. Southw. Symp. Image Anal. Interpret. 12 (1998), 154–159.
- [4] C. Pozrikidis, Resting shape and spontaneous membrane curvature of red blood cells, IMA J. Math. Med. Biol. 22 (2005), 34–52.
- [5] L. C. Evans, Partial Differential Equations, American Mathematical Society, Providence, Rhode Island, 2000.
- [6] Q. Du, L. Ju, X. Li, and Z. Qiao, Maximum bound principles for a class of semilinear parabolic equations and exponential time differencing schemes, SIAM Rev. 63 (2021), 317–359.
- [7] L. C. Evans, H. M. Soner, and P. E. Souganidis, *Phase transitions and generalized motion by mean curvature*, Commun. Pure Appl. Math. 45 (1992), 1097–1123.
- [8] J. H. Bramble and B. E. Hubbard, *New monotone type approximations for elliptic problems*, Math. Comput. 18 (1964), 349–367.
- [9] P. G. Ciarlet, Discrete maximum principle for finite-difference operators, Aequationes Math. 4 (1970), 338–352.
- [10] J. H. Brandts, S. Korotov, and M. Krzek, *The discrete maximum principle for linear simplicial finite element approximations of a reaction-diffusion problem*, Linear Algebra Appl. 429 (2008), 2344–2357.
- [11] S. Badia and A. Hierro, *On discrete maximum principles for discontinuous Galerkin methods*, Comput. Methods Appl. Mech. Eng. 286 (2015), 107–122.
- [12] E. G. Yanik, A discrete maximum principle for collocation methods, Comput. Math. Appl. 14 (1987), 459–464.
- [13] E. G. Yanik, Sufficient conditions for a discrete maximum principle for high order collocation methods, Comput. Math. Appl. 17 (1989), 1431–1434.
- [14] G. Yuan and Y. Yu, Existence of solution of a finite volume scheme preserving maximum principle for diffusion equations, Numer. Meth. Part. Diff. Eq. 34 (2018), 80–96.
- [15] P. Stehlk and J. Volek, Maximum principles for discrete and semidiscrete reaction-diffusion equation, Discrete Dyn. Nat. Soc. 2015 (2015), 791304.
- [16] T. Tang and J. Yang, *Implicit-explicit scheme for the Allen-Cahn equation preserves the maximum principle*, J. Comput. Math. 34 (2016), 471–481.
- [17] J. Shen, T. Tang, and J. Yang, On the maximum principle preserving schemes for the generalized Allen-Cahn equation, Commun. Math. Sci. 14 (2016), 1517–1534.
- [18] J. Rubinstein and P. Sternberg, *Nonlocal reaction-diffusion equations and nucleation*, IMA J. Appl. Math. 48 (1992), 249–264.
- [19] J. Li, L. Ju, Y. Cai, and X. Feng, Unconditionally maximum principle preserving linear schemes for the conservative Allen-Cahn equation with nonlocal constraint, J. Sci. Comput. 87 (2021), 98.
- [20] M. Brassel and E. Bretin, A modified phase field approximation for mean curvature flow with conservation of the volume, Math. Methods Appl. Sci. 34 (2011), 1157–1180.
- [21] M. Alfaro and P. Alifrangis, Convergence of a mass-conserving Allen-Cahn equation whose Lagrange multiplier is nonlocal and local, Interfaces Free Bound. 16 (2014), 243–268.

- [22] J. Kim, S. Lee, and Y. Choi, A conservative Allen-Cahn equation with a space-time dependent Lagrange multiplier, Int. J. Eng. Sci. 84 (2014), 11–17.
- [23] S. Zhai, Z. Weng, and X. Feng, *Investigations on several numerical methods for the non-local Allen-Cahn equation*, Int. J. Heat Mass Transf. 87 (2015), 111–118.
- [24] S. Zhai, Z. Weng, and X. Feng, Fast explicit operator splitting method and time-step adaptivity for fractional non-local Allen-Cahn model, Appl. Math. Model. 40 (2016), 1315–1324.
- [25] H. G. Lee, High-order and mass conservative methods for the conservative Allen-Cahn equation, Comput. Math. Appl. 72 (2016), 620–631.
- [26] G. Beylkin, J. M. Keiser, and L. Vozovoi, A new class of time discretization schemes for the solution of nonlinear PDEs, J. Comput. Phys. 147 (1998), 362–387.
- [27] S. M. Cox and P. C. Matthews, Exponential time differencing for stiff systems, J. Comput. Phys 176 (2002), 430–455.
- [28] M. Hochbruck and A. Ostermann, Explicit exponential Runge-Kutta methods for semilinear parabolic problems, SIAM J. Numer. Anal. 43 (2005), 1069–1090.
- [29] M. Hochbruck and A. Ostermann, Exponential integrators, Acta Numer. 19 (2010), 209–286.
- [30] Q. Du and W. Zhu, Stability analysis and application of the exponential time differencing schemes, J. Comput. Math. 22 (2004), 200–209.
- [31] Q. Du and W. Zhu, Analysis and applications of the exponential time differencing schemes and their contour integration modifications, BIT Numer. Math. 45 (2005), 307–328.
- [32] L. Ju, J. Zhang, L. Y. Zhu, and Q. Du, Fast explicit integration factor methods for semilinear parabolic equations, J. Sci. Comput. 62 (2015), 431–455.
- [33] L. Ju, J. Zhang, and Q. Du, Fast and accurate algorithms for simulating coarsening dynamics of Cahn-Hilliard equations, Comput. Mater. Sci. 108 (2015), 272–282.
- [34] X. Q. Wang, L. Ju, and Q. Du, Efficient and stable exponential time differencing Runge-Kutta methods for phase field elastic bending energy models, J. Comput. Phys. 316 (2016), 21–38.
- [35] W. Chen, W. Li, Z. Luo, C. Wang, and X. Wang, A stabilized second order ETD multistep method for thin film growth model without slope selection, EASIM Math. Model. Num. Anal. 54 (2020), 727–750.
- [36] K. Cheng, Z. Qiao, and C. Wang, A third order exponential time differencing numerical scheme for no-slope-selection epitaxial thin film model with energy stability, J. Sci. Comput. 81 (2019), 154–185.
- [37] J. Zhang, C. Zhou, Y. Wang, L. Ju, Q. Du, X. Chi, D. Xu, D. Chen, Y. Liu, Z. Liu, Extreme-scale phase field simulations of coarsening dynamics on the Sunway TaihuLight supercomputer (Proc. Int. Conf. High Perform. Comput. Network. Storage Anal.), Article #4. IEEE Press, 2016.
- [38] T. Hou, T. Tang, and J. Yang, Numerical analysis of fully discretized crank-Nicolson scheme for fractional-in-space Allen-Cahn equations, J. Sci. Comput. 72 (2017), 1214–1231.
- [39] Q. Du, L. Ju, X. Li, and Z. Qiao, Maximum principle preserving exponential time differencing schemes for the nonlocal Allen-Cahn equation, SIAM J. Numer. Anal. 57 (2019), 875–898.
- [40] L. Ju, X. Li, Z. Qiao, and J. Yang, Maximum bound principle preserving integrating factor Runge-Kutta methods for semilinear parabolic equations, J. Comput. Phys. 439 (2021), 110405.
- [41] J. Li, X. Li, L. Ju, and X. Feng, Stabilized integrating factor Runge-Kutta method and unconditional preservation of maximum bound principle, SIAM J. Sci. Comput. 43 (2021), A1780–A1802.
- [42] H. Zhang, J. Yan, X. Qian, X. Gu, and S. Song, On the preserving of the maximum principle and energy stability of high-order implicit-explicit Runge-Kutta schemes for the space-fractional Allen-Cahn equation, Numer. Algor (2021), 1–28. https://doi.org/10.1007/s11075-021-01077-x
- [43] B. Li, J. Yang, and Z. Zhou, Arbitrarily high-order exponential cut-off methods for preserving maximum principle of parabolic equations, SIAM J. Sci. Comput. 42 (2020), A3957–A3978.
- [44] Y. Hao, Q. Huang, and C. Wang, A third order BDF energy stable linear scheme for the no-slope-selection thin film model, Commun. Comput. Phys. 29 (2021), 905–929.
- [45] W. Rudin, Principles of mathematical analysis, McGraw-Hill Cooperation, New York, 1964.

How to cite this article: K. Jiang, L. Ju, J. Li, and X. Li, *Unconditionally stable exponential time differencing schemes for the mass-conserving Allen–Cahn equation with nonlocal and local effects*, Numer. Methods Partial Differ. Eq. (2021), 1–22. https://doi.org/10.1002/num.22827